Biophysical study of *Brucella abortus* on electrochemical platform

[1]Ajay Kumar Gupta, [2] V. K. Rao, [3] D.T Selvam

Scientists
Centre of Excellence for Advanced Materials, Manufacturing, Processing and Characterization
Vignan's Foundation for Science Technology & Research University, Guntur-522213, India

Abstract-Study of biophysical interactions have been carried out using specific combination of proteins such as *Brucella abortus* cell envelop protein (as antigen) and its complementary antibody (raised in mice and rabbit). A best optimized composition of biocompatible CeO_2 nano-octahedra and other biocompatible materials (chitosan) was used in this study. Linear range was found in the range of 6.25 µg/mL–100 µg/mL. Detection limit was found 0.1 ng/mL. By conventional plate ELISA it was possible to detect 50 µg/mL only. Experiments were conducted using 110 suspected patient serum samples and results were compared with ELISA and Rose Bengal Plate test (RBPT). We also studied the shelf life of prepared immunosensor. The shelf life of immunosensor was found to be 51 days.

***Index Term*: Biophysics; Electrochemistry, ELISA; CeO_2 nano-octahedra; CE-protein antigen**

***Abbreviation:* Ch, chitosan; GCE, Glassy carbon electrode; CE-protein antigen, Cell envelope protein antigen; ELISA, enzyme linked immunosorbent assay; RBPT, Rose Bengal Plat Test, PCR, Polymerase chain reaction; CAb, capturing antibody; RAb, revealing antibody; ALP, alkaline phosphatase; PBS, phosphate buffer saline; DEA, Diethanolamine; LPS, lipopolysaccharide; CV, Cyclic Voltammetry. PNPP, *p*-nitro phenyl phosphate, O.D., optical Density.**

I. INTRODUCTION

Highly specific immunoassay technique for recognition of antigen by its specific antibody have become the electro-analytical methods in clinical diagnosis and biochemical analysis [1-5]. Electrochemical immunosensors combine the high specificity of traditional immunochemical methods with the low detection limit of a modern electrochemical system. Whereas, conventional immunoassay methods such as enzyme linked immuno sorvent assay (ELISA) is comparatively less sensitive, requires more time for analysis, complicated wash procedure, expensive, cumbersome instruments and requires skillful manpower [6-8]. Thus, electrochemical immunosensor is much more useful regarding performance. However, there are certain limitations with respect to electro-catalytic activity towards analytes and low adsorption of biomolecules. Therefore several authors used nanomaterials, biocompatible materials and electro-catalysts in development of biosensor [9-13]. In this biophysical study, we used alkaline phosphatase (ALP) and it is reported that electrochemical method is better than conventional ELISA methods developed using alkaline phosphatase (ALP) [14]. In case of electrochemical immunosensing, it is also possible to miniaturize the electrode for field applications [15].

Brucella abortus is gram negative and intracellular micro-organism. It causes brucellosis disease which is zoonotic in nature, and hence, it can be transferred from cattle to a human and remains pathogenic. The bacteria are transmitted by contact with infected animal, ingestion of infected milk, milk products and inhalation of aerosols. This disease rarely transmitted from mother to child in case of human. Brucellosis is considered by FAO, WHO and O I E as the most widespread zoonosis in the world. The prevalence of this disease is very high in India [16].

The lipopolysaccharide (LPS) of smooth *Brucella* species is the strongest antigen compared to other antigenic molecules and has been considered as the most important antigen as it elicits strong and long lasting immune response in brucellosis [17,18]. Cell Envelope (CE) protein is an outer membrane protein of *B. abortus* and the molecular weight of immunogenic CE-protein antigen varies from 11.8 kDa to 110.8 kDa [19]. Several standard tests such as standard plate agglutination test, standard tube agglutination test, acidified plate antigen test, rivanol precipitation plate antigen test, serial dilution milk ring test, complement fixation test, standard buffered brucella antigen card test, mercaptoethanol agglutination test and ELISA have been used in the diagnosis of brucellosis [20]. These tests are mainly based on the detection of antibodies directed against the lipopolysaccharide portion of the cell membranes. Tests are also available for the detection of *Brucella* antigen. Al-Shamahy et al. reported enzyme linked immunosorbent assay for *Brucella* antigen detection in human sera [21]. Al-Farwachi et al. also reported modified ELISA test for detection of *Brucella* antigen in the aborted ovine fetal stomach content [22]. Immuno-histochemical technique and polymerase chain reaction (PCR) were also carried out for detection of *Brucella* infection [23,24]. Several methods were reported in the literature for detection of brucellosis in recent years. However, these methods are either time-consuming and/or of low in sensitivity. Some of the methods require highly qualified personnel (e.g., PCR) or sophisticated instrumentation (PCR, florescence microscopy, and flow cytometry) [25-27]. The requirement of highly qualified manpower and sophisticated instrumentation make them less useful in the diagnosis.

Among nanomaterials, metal oxides have been found to exhibit high surface-to-volume ratio, high surface reaction activity, high catalytic efficiency and strong adsorption ability which make them potential materials for the fabrication of biosensor [28-34]. Among these nanostructures, CeO_2 have aroused much interest for development of implantable biosensors due to high

mechanical strength, low temperature processing tunability in physical parameter, chemical inertness, oxygen ion conductivity, biocompatibility, oxygen storage capacity, nontoxicity, high chemical stability, negligible swelling in aqueous and non-aqueous solutions for the immobilization of biomolecules and high electron transfer. Moreover, high iso-electric point (IEP) of CeO_2 (9.2) can be helpful to immobilize desired bio-molecules of low IEP *via* electrostatic interactions [35-42]. CeO_2 was widely used in electro-catalytic oxidation of various analytes [43-45].

In this study, the prepared CeO_2 was nano-porous in nature. Since, the size of individual intact antibodies (IgG) is also in nanometer range [46], and hence, CeO_2 may trap more quantity of IgG molecules and hence provide biocompatible micro-environment to IgG molecules. All these properties of prepared CeO_2 in this study were helpful to achieve very high sensitivity and good shelf life of immunosensor. Thus we attempted to use this potential material in such immunosensing application wherein the oxidation product of 1-naphthol was directly related to the sensitivity of immunosensor. In one of our earlier report, we have done a small study limited to amperometry on bare screen printed electrode without any kind of modification [47].

In this present study, we attempted to improve bio-sensing characteristics of immunosensor by dispersing nano CeO_2 in biopolymer e.g. chitosan to fabricate nano-biocomposite. Chitosan has been explored for biosensor development [29] due to its excellent film forming ability, mechanical strength, biocompatibility, nontoxicity, susceptibility to chemical modification and cost effectiveness. Moreover, amino groups of Ch provide a hydrophilic environment compatible with the biomolecules [48]. In order to enhance the shelf life of immunosensor in the best way, we optimized first the chitosan concentration and then mixed with nano-octahedra CeO_2 in that best optimized proportion.

In this present study, we observed post-zone phenomenon, cause of false negative reaction. For the detection of antigen-antibody complex formation, the ratio between antigen and antibody is the influencing factor. When antigens and antibodies are in optimum ratio, lead to cross linkage and hence agglutination appears, resulting in positive reaction. But when antigen concentration become in excess (post-zone phenomenon), agglutination is hidden by mass of unagglutinated antigens and resulted in false negative reaction. This phenomenon is known as post-zone phenomenon. Yorgancigil et al. diluted the specimens to avoid post-zone effect in detection of Brucella infection [49]. These false-negative reactions can be detected by higher dilutions of antigen sample, which reduces the antigen concentration into the range that produces visible agglutination. In this present study, we observed post-zone like phenomena with electrochemical immunosensor. However, no false negative result was observed. Also the sensitivity of immunosensor was much higher than ELISA.

II. MATERIALS AND METHODS

Apparatus

Cyclic voltammetry (CV) experiments and chrono amperometric experiments were performed with a CH Instrument, 440A. The detection was carried out in a 10 mL electrochemical cell, with GCE as a working electrode; an Ag/AgCl/Satd. KCl was used as reference electrode with platinum wire as a counter electrode. Nano-spectrophotometer (Implen) has been used for finding change in absorbance. Sonication has been done by using Sonics & Materials Inc., model no. VCX 750. SEM (Quanta 400 ESEM The Netherlands) has been used for scanning electron micrograph (SEM) studies. Raman study was carried out by using Renishaw Invia Raman Microscopy and surface area was calculated by using Micromeritics, USA, ASAP 2020 instrument.

Reagents and chemicals

Cerium chloride ($CeCl_3.7H_2O_2 \geq 99.0\%$), formamide ($HCONH_2$, $\geq 99.5\%$), and polyvinylpyrrolidone (PVP), hydrogen peroxide (H_2O_2, 30%) were required for synthesis of nano-octahedra CeO_2. The detection buffer consisted of 0.1 M diethanolamine (DEA) containing 0.02 M of magnesium chloride and 0.1M sodium chloride (NaCl) with an adjusted pH of 9.8. The antigen/antibody buffer consisted of 0.02 M phosphate buffer with 150 mM NaCl (PBS pH 7.4). It has been reported that pH 7.4 was best optimized for the antibody immobilization [49]. The washing buffer consisted of 100 mM of Tris and 100 mM NaCl and adjusted to pH 7.2. Standard solution of the CE-protein antigen was prepared (0.5 mg/mL) in PBS of pH 7.4 and the required dilutions were made as and when required. Anti-*B. abortus* CE-protein antibody was raised in mice (CAb) and anti-*B. abortus* CE-protein antibody was raised in rabbit and conjugated to ALP as per standard protocols in our laboratory. CAb and RAb were diluted using 100 mM Tris containing 100 mM NaCl with a pH 7.4. The dilutions were prepared freshly before use. In spectroscopic study, *p*-nitro phenyl phosphate (PNPP) was used as a substrate of ALP. Cerium chloride, formamide, PVP, H_2O_2, BSA, DEA, 1-napthyl phosphate monosodium salt, PNPP, Tris–HCl, PBS buffer was purchased from Sigma Chemicals. Other chemicals used were of analytical grade.

Preparation of Nano-octahedra CeO_2

Nano-octahedra CeO_2 was prepared by hydrothermal method [50,51]. In a typical synthesis of CeO_2 hollow nanospheres, 0.396 g of $CeCl_3.7H_2O$ and 0.712 g of PVP were dissolved in 76 mL of deionized water under vigorous magnetic stirring. 4 mL of formamide and 0.4 mL of H_2O_2 were then added into the solution under continuous stirring for 30 min. The as formed yellow solution was transferred into a teflon-lined autoclave of 100 mL capacity and heated for 24 h at 180 $^{\circ}$C. After the autoclave was cooled naturally to room temperature, light brown products were collected and washed with deionized water 4 times. Finally the products were washed with absolute ethanol and dried in an electric oven for 6 h at 70 $^{\circ}$C.

Appropriate amount of nano-octahedra CeO_2 was dispersed in 0.5% of Chitosan (0.05 mM acetic acid). The mixture was sonicated for 15 min after stirring for 1 h. Finally a highly dispersed solution was formed. A volume of 10 µL resulting highly dispersed solution was pipetted onto GCE. The solution was allowed to dry at room temperature. Various mass ratios of nano-octahedra CeO_2:Ch were used to modify the GCE. These modified electrodes were characterized by cyclic voltammetry with ferrocyanide/ferrocyanide redox couple and also conducted with 1-naphthol. The composition of 85:15 ratio was found to be best.

This mass ratio of nano-octahedra CeO_2 and chitosan gave least potential separation among all mass ratios of nano-octahedra CeO_2 and chitosan.

CE-protein preparation

B. abortus S99 bacterial strain regularly maintained in the laboratory in 20% glycerol stock was revived in 5 mL BHI broth at 37 °C for overnight. 3 mL of overnight grown culture was inoculated into 300 mL of BHI broth and incubated in an incubator shaker at 37 °C with constant shaking (180 rpm). Bacterial cells were then harvested after inactivating the cells by formaldehyde treatment for 1 h. The bacterial pellet obtained was washed twice with sterile PBS and resuspended into 100 mL of buffer 1, pH 8.0 (Tris–HCl 15 mM, Sucrose 0.45 mM, EDTA 8 mM, lysozyme 0.4 mg/mL). The bacterial suspension was incubated in water bath at 47 °C for 15 min and then centrifuged at 10000 rpm for 15 min. Pellets were resuspended in 10-15 mL buffer 2, pH 7.6 (Tris–HCl 50 mM, $MgCl_2$ 5 mM, PMSF 2 mM). Further bacterial suspension was sonicated by using Vibrocell (Sonics) sonicator. The bacterial suspension was placed in crushed ice to prevent degradation of protein and 5 cycles of 5 min each with a pulse after every 8 sec and amplitude at 40 W was given for the complete sonication of bacterial cells. The sonicated suspension was centrifuged at 6000 rpm for 30 min at 4 °C. Supernatant was collected and subjected to ultra centrifugation at 43500 rpm at 4 °C for 90 min (Sorvall ultra pro). The obtained pellets were then resuspended finally in 1.5 mL of buffer 3 of pH 7.6 (Tris–HCl 50 mM, PMSF 2 mM), and again centrifuged at 10000 rpm for 10 min and the supernatant was stored at -20°C. The protein concentration was estimated by Lowry et al. [52] and found to be 0.5 mg/mL. In addition to this the protein was also characterized by SDS-PAGE [19].

Raising of Antibody

Polyclonal antibodies against CE-protein antigen were raised in rabbit and mice. First dose of CE-protein was given at a concentration of 20-30 µg per mice and 500 mg/rabbit with Frund's complete adjuvant (Difco). Four booster doses were then given at an interval of 7 days with incomplete Frund's adjuvant (Difco). The animals were regularly bled and serum was collected after 7 days to check the antibody titre by plate ELISA. The animals were finally bled and serum was pooled with a titre of 1:51,200 in mice and1:1,20,000 in rabbit. The serum containing polyclonal antibodies against CE-protein antigen was stored at -20 °C in aliquots for further use. The rabbit sera was further subjected to IgG purification and purified IgG was conjugated to alkaline phosphatase by using standard procedure. This polyclonal antibody raised in mice was used as capture antibody and the alkaline phosphatase tagged rabbit polyclonal antibody was used as revealing antibody in immunosensor. The generation of antibodies in animals used in this study has been approved by institutional animal ethics committee.

Steps in immunosensing of CE-protein antigen

A sandwich ELISA method as depicted in Schematic diagram (graphical abstract) was used. A known quantity (10 µL) of CAb of CE-protein antigen in PBS buffer was physically adsorbed on the nano-octahedra CeO_2/Ch/GCE. It was left at 37 °C for 1 h. Subsequently it was blocked with buffered solution of 3% BSA for 30 min. This will reduce the nonspecific adsorption effect. Later the electrodes were incubated with the dilute concentrations of CE-protein antigen in PBS solution for 15 min. This results in selective antigen antibody interaction. Electrodes were further incubated with revealing antibody for 15 min. The secondary antibodies (RAb) form a complex with the secondary sites forming a sandwich ELISA assay [53]. After each step the electrodes were washed with Tris buffer containing NaCl at pH 7.2 to remove any unbound antigen or antibody. The electrode was finally dipped in an electrochemical cell containing DEA buffer (pH 9.8) and a potential of 0.30 V with respect to reference Ag/AgCl/Satd. KCl electrode was applied. After allowing 200 s for the stabilization of the electrode to achieve constant current, the substrate 1-napthyl phosphate was added and the resulting amperometric current was noted. The output current obtained can be co-related to the concentration of CE-protein present on the electrodes.

II. RESULTS AND DISCUSSION

Physical characterization of Nano-octahedra CeO_2

Figure 2 shows the SEM image of as prepared nano-octahedra CeO_2, in which morphology was investigated. This figure shows the uniform spheres. These spheres were constructed by the uniform nano-octahedra.

Surface area, pore size and pore volume study

Surface Area analysis

In as prepared nano-octahedra CeO_2, the single point surface area at p/p^o of 0.31 was 72.16 m^2/g. BET surface area was found to be 73.1 m^2/g whereas Langmuir surface surface area was 105.71 m^2/g. In the surface area analysis, BJH adsorption cumulative surface area of pores between 1.7 nm and 300 nm width was 78.28 m^2/g whereas BJH desorption cumulative surface area of pores between 1.7 nm and 300 nm width was 88.42 m^2/g.

Pore Volume and Pore Size analysis

In the pore volume analysis of as prepared nano-octahedra CeO_2, single point adsorption total pore volume of pores at width of less than 100.94 nm and p/p° of equal to 0.98 was 0.16 cm^3/g. BJH Adsorption cumulative volume of pores between 1.7 nm and 300 nm width was found to be 0.15 cm^3/g whereas BJH Desorption cumulative volume of pores between 1.7 nm and 300 nm width was 0.15 cm^3/g.

In pore size analysis of as prepared nano-octahedra CeO_2, BET adsorption average pore width (4V/A) was found to be 8.65 nm whereas BJH adsorption average pore width (4V/A) was found to be 7.69 nm and BJH desorption average pore width (4V/A)

was found to be 6.98 nm. This pore width is comparable to the size of IgG (8.6 nm for individual intact rabbit IgG). Hence, the antibodies can be trapped in the pores of nano CeO_2 and thus more quantity of antibodies can be adsorbed on the CeO_2/Ch/GCE compared to GCE which has no pores. From these observations, it can be concluded that this materials has nanopores which can help in trapping the biomolecules. Also the biomolecules may be trapped in the voids present among nano-octahedra CeO_2.

Electrochemical optimization of Nano-octahedra CeO_2 composition with chitosan

Various compositions of nano-octahedra CeO_2 and 0.5% Chitosan solution in the ratio of 50:50, 70:30, 85:15, and 95:05 were prepared and used to modify GCE. The nano-octahedra CeO_2/Ch/GCE was studied with standard redox couple (1 mM of ferricyanide/ferrocyanide redox couple in PBS) by cyclic voltammetry (CV) (Fig. 2a). It should be noted that in each cyclic voltammetry (CV) experiment of Fig. 2(a) same redox couple ($[Fe(CN)_6]^{-3/-4}$) and same electrochemical interface (CeO_2/Ch composite modified GCE) was used. And this is reason that peaks in cyclic voltammetry (CV) graphs in Fig. 2(a) are present on the approximately same reduction/oxidation potential or the peaks having small difference in reduction/oxidation potentials.

It was observed that as we increased the ratio of nano-octahedra CeO_2 (which is consider for increasing the electron transfer rate) in the composition of nano-octahedra CeO_2 and chitosan, the current increased continuously up to the compositions of 85:15. When we further increased the ratio of CeO_2 to 95:05, peak current was slightly less than the peak current of 85:15 composition. Thus composition (85:15) of nano-octahedra CeO_2 and chitosan was optimized for further study. Figure 2(a) shows the optimization of composition ratio of nano-octahedra CeO_2 and chitosan. The ΔE value at the composition of 85:15 found to be 102 mV. This value differs from ideal value (59.1 mV) due to use of binder material (chitosan) which reduces the electron transfer rate.

By using this optimized ratio, the average value of the electroactive surface area was calculated according to the Randles–Sevick equation

$$Ip = 2.69 \times 10^5 \, AD^{1/2} \, n^{3/2} \, \gamma^{1/2} \, C$$

where n is the number of electrons participating in the redox reaction (in case of ferricyanide/ferrocyanide redox couple n=1), A is the area of the electrode (cm^2), D is the diffusion coefficient of the molecule in solution ($cm^2\ s^{-1}$) (in case of ferricyanide/ferrocyanide redox couple D =7.6 x 10^{-6} $cm^2\ s^{-1}$), C is the concentration of the probe molecule in the bulk solution (mol cm^{-3}), and γ is the scan rate (mV s^{-1}). The electro-active surface area for CeO_2 modified GCE and bare GCE was 1.627 x 10^{-2} cm^2 and 3.887 x 10^{-3} cm^2. Evidently the modified electrode had increased electro-active surface area which is nearly 4.18 times to bare GCE.

In the same fashion various composition ratios of CeO_2 and chitosan were again optimized by means of CV of nano-octahedra CeO_2 /Ch/GCE in 0.5 mM of 1-naphthol (prepared in DEA buffer) (Fig.2b). It was observed that as we increased the ratio of nano-octahedra CeO_2 in the composition of nano-octahedra CeO_2 and chitosan, the oxidation current of 1-naphthol increased continuously up to the compositions of 85:15. When we further increased the ratio of CeO_2 to 95:05, oxidation current of 1-naphthol was found less than that of 85:15 composition. And hence, we optimized this 85:15 composition of nano-octahedra CeO_2 and Chitosan for further experiments.

Electrochemical characterization of Nano-octahedra CeO_2

Nano-octahedra CeO_2 modified GCE was electrochemically characterized with 0.5 mM 1- naphthol (prepared in DEA) (Fig. 2c) and showed that nano-octahedra CeO_2 modified GCE was electrochemically more sensitive than bare GCE.

In Fig. 2(d), amperometric response of nano-octahedra CeO_2/Ch/GCE shows its more stability as well as sensitivity in comparison to bare GCE towards constant and subsequent addition of 1-naphthol in 10 mL of DEA at constant voltage of 0.30 V. Porous nature of CeO_2 enhances the capacity to trap the secondary antibody conjugated to ALP (RAb), and hence, causes more hydrolysis of 1-naphthyl phosphate (substrate of ALP enzyme), which need to be measured in amperometric response. Thus the CeO_2/Ch/GCE should have higher sensitivity.

In Fig. 2(c), the oxidation peak potential of 1-naphthol on bare GCE was 0.35 V vs. Ag/AgCl. While on CeO_2/Ch/GCE, it was 0.29 V vs. Ag/AgCl. This cathodic shift in oxidation potential clearly indicates the electro-catalytic activity of CeO_2 towards 1-naphthol. Moreover, the response of CeO_2/Ch/GCE (23.3 μA) is much higher than at bare GCE (6.9 μA) electrode. Thus the current was enhanced 3.37 times on the GCE due to CeO_2. The same was reflected in the amperometric response of as shown in Fig. 2(d). The enhancement in amperometric current was 3.37 times comparing to GCE. This enhancement in response of GCE was comparable to increase in electrochemical surface area of GCE due to CeO_2 as found by using $[Fe(CN)_6]^{-3/-4}$ redox couple. The difference between enhancement of the current of redox couple $[Fe(CN)_6]^{-3/-4}$ and 1-naphthol on CeO_2/Ch modified GCE was due to reversible nature of redox couple and irreversible nature of 1-naphthol.

Relative adsorption efficiency of Nano-octahedra

In order to investigate the relative adsorption efficiency of nano-octahedra CeO_2/Ch/GCE, spectroscopic experiments were carried out (Fig.3a).

For this study, RAb (1:100) was adsorbed on these electrodes for 15 min, and then washed with washing buffer (Tris buffer pH 7.2 was used). Electrodes were exposed to 2 mL of 4 mM p-nitro phenyl phosphate (PNPP) substrate. This is a substrate for ALP. Optical density (O.D.) of this solution was noted at various intervals of time. These adsorption efficiencies of CeO_2/Ch/GCE at various intervals of time were compared with that of screen printed electrode (SPE), MWCNT-paste electrode and ZnO modified SPE (Fig. 3a). We observed that adsorption efficiency of CeO_2/Ch/GCE was best among all the compared electrodes. This can be attributed to high RAb adsorption efficiency of nano-octahedra CeO_2 having nano-size cavities. Higher the

adsorption of RAb, higher will be the sensitivity. At pH 7.2, CeO_2 has positive charge due to its high IEP value (9.2) and polyclonal antibodies have negative charge due to low IEP value (≥ 4) and hence, resulted into high adsorption efficiency towards ALP conjugate antibody (revealing antibody). Physical adsorption process was carried out at pH 7.2.

Electrochemical Impedance spectroscopic study

EIS was employed to characterize the interface properties of the modified electrodes (in our case chitosan modified GCE and nano-octahedra CeO_2/Ch/GCE). In a typical Nyquist plot, the semicircle portion correspond to the electron-transfer resistance (R_{et}.) at higher frequency range while a linear part at lower frequency range represents the diffusion limited process. In this report, EIS study of the electrodes was carried out in 1 mM $[Fe(CN)_6]^{3-/4-}$ containing 0.1 M KCl solution with a frequency range of 0.01 Hz–10 kHz.

As shown in Fig. 3(b), Curve (a) represents the spectra of unmodified GCE. After immobilization of chitosan (curve b), the semicircle domain of Nyquist plot increased suggesting that chitosan layer blocked the redox probe to diffuse toward the electrode surface. Semicircle domain decreases dramatically for the nano-octahedra CeO_2/Ch modified GCE (curve c) suggesting that nano-octahedra CeO_2/Ch modified GCE have excellent electro-catalytic activity and it makes high electron conduction pathways between the electrode and electrolyte.

IR study

Composition and quality of the prepared nano-octahedra CeO_2 were analyzed by IR spectroscopy. In the IR spectra of nano-octahedra CeO_2, strong band at 3435 cm^{-1}, 1589 cm^{-1} and below 700 cm^{-1} were observed (figure is not shown). The intense band at 3435 cm^{-1} and 1589 cm^{-1} correspond to the ν (O-H) mode of (H-bonded) water molecules and δ (O-H), respectively [54]. The IR spectrum of the cerium also exhibit strong band below 700 cm^{-1} which is due to the δ (Ce-O-Ce) mode.

Raman study

In the Raman spectra of nano-octahedra CeO_2 (figure is not shown), there are single peaks at about 462 cm^{-1} which represents the optical Raman active E_{2g} symmetry mode, which originates from oxygen stretching vibrations and can be viewed as a symmetric breathing mode of the O atoms around each cation. Since only the O atoms move, vibrational mode is nearly independent of the cation mass [55,56].

Optimization of revealing antibody (RAb)

In the optimization process of RAb, nano-octahedra CeO_2/Chitosan composite GCEs were blocked with BSA for 30 min and then incubated with RAb for 15min. Various dilutions of RAb were incubated and tested for obtaining the blank current. There was an appreciable increase in background current when a dilution of 1:20,000 to 1:100 was used. This background current is due to nonspecific adsorption of RAb on sensing surface. A dilution of 1:10,000 of the RAb was optimized for further studies. Optimization of RAb is shown in fig. 4.

Optimization of capture antibody (CAb)

For the optimization of CAb, all the steps except the step of incubation of the antigen were performed. There was no nonspecific interaction (CAb–RAb interaction). The amperometric current almost matched with the blank current obtained with 1:10,000 dilution of RAb. So CAb was used as such without diluting for further experiments.

Detection of CE-protein antigen

In electrochemical detection process, nano-octahedra CeO_2/Chitosan composite GCE was initially incubated with CAb at optimized dilution for 60 min. Subsequently, that was blocked with 3% BSA for 30 min followed by incubation in CE-protein antigen at various concentrations. Then these electrodes were incubated with RAb for 15 min. Each step is followed by washing with washing buffer to remove any unbound antigen or antibodies. These electrodes were dipped in an electrolyte containing DEA buffer at pH 9.8. A potential of 0.30 V vs. Ag/AgCl was applied and the amperometric current was measured. When the current reached a steady state value, the substrate is added and the rise in the current was noted. The amperometric response was found to be linear in the concentration range of 6.25 µg/mL to100 µg/mL (Fig. 5a). A linear dependence of the current response on the concentration of antigen over the range from 6.25 µg/mL to100 µg/mL was obtained with a regression equation of i (nA) = 34.12 + 2.448 x antigen (µg/mL) (R^2=0.999) for the CeO_2/Ch/GCE (Fig. 5a). Detection limit was found to be 0.1 ng/mL (Fig. 5b).

Calibration plots (Fig. 5a & Fig. 5b) are the result of mean values of 3 times replicates for each concentration of antigen. The reproducibility of the immunosensor was evaluated from the amperometric response to 50 ng/mL of antigen using different nano-octahedra CeO_2/Ch/GCEs and the relative standard deviation was found to be 6.7%. Figure 5(b) shows high response at low concentrations. This can be attributed to post-zone like effect. In general, the pro-zone like effect is found in detection of antibodies of Brucella in agglutination test [57,58]. By means of plate ELISA test and other test, pro-zone like effect were also reported in *Salmonella, E. coli, Leptospira hadjo* etc. [59-62]. Here we observed post-zone like effect. The post-zone like effect was observed in detection of *Brucella* antigen, *hepatitis B* antigen and *Francisella tularensis* antigen [63-65]. The false negative results of agglutination test were attributed to this phenomenon. The immunosensor does not give false negative results even at high concentration of the antigen. The high sensitivity of nano-octahedra CeO2/Ch/GCE can be attributed to good electrochemical behavior and high adsorption efficiency. We successfully tested the immunosensor with 110 patient serum samples.

Patient Serum sample detection

110 patient serum samples were also tested amperometrically by using nano-octahedra CeO_2 modified GCEs and compared those results with plate ELISA [66] and RBPT [67]. Samples used for the electrochemical immunosensor, ELISA and RBPT were same. Furthermore, the patient samples were diluted 10 times and the results were presented in **TABLE 1.** It was found that even after diluting the samples 10 times, the immunosensor was able to detect, while ELISA & RBPT were unable to detect the diluted samples. These results showed that the sensitivity of electrochemical immunosensor was much better than ELISA and RBPT test. Criteria of the judgment about positive or negative for electrochemical immunosensor were determined on the basis of the equation **[baseline current (blank current) + 3 X standard deviation (S.D.)].** In ELISA, positive and negative was explained on the basis of change in O.D. (optical density). While in case of RBPT, positive and negative was explained on the basis of agglutination. A complete agglutination with equal volume of antigen was determined as positive result for RBPT. In table 1, there were also some unclear samples. Unclear samples were those samples which have the response very close to the value obtained from the equation **[baseline current (blank current) + 3 X standard deviation (S.D.)].** Thus it is very difficult to determine these samples as positive or negative and hence, kept these samples in a separate category of **unclear samples**. It may be noted that these unclear samples were found negative in case of ELISA and RBPT even after dilution by 10 times.

In this study, we observed post-zone phenomenon which may be the one of the most important reason of this considerable difference in the no. of positive samples obtained from electrochemical techniques and other techniques such as RBPT and ELISA. Due to post-zone phenomenon, there is a high probability of occurrence of false negative results. And this may be the reason that in this study, we observed a large number of negative samples in RBPT and ELISA test. These biological techniques such as RBPT and ELISA are based on agglutination reaction between antigen and antibody. A complete agglutination with equal volume of antigen was determined as positive result. This agglutination reaction is hidden by mass of unagglutinated antigens in case of post-zone phenomenon (observed in this study) and thus resulted in false negative reaction.

Thermal stability study of immunosensor

The shelf life of immunosensor is one important aspect of immunosensor. Hence, thermal stability of immunosensor was also studied at various temperatures (4 $^{\circ}$C, 37 $^{\circ}$C and 50 $^{\circ}$C). For this study, initially the electrodes were treated with optimized concentration of CAb and 3% BSA as detailed in experimental section (steps in immunosensing of CE-protein antigen) and stored these electrodes at various temperatures such as 4 $^{\circ}$C, 37 $^{\circ}$C and 50 $^{\circ}$C. Prior to experiments, electrodes were further treated with antigen (25 ng/mL) for 15 min and then with optimized concentration of RAb for 15min. Electrodes stored at 50 $^{\circ}$C, lost activity within 2 day and electrodes stored at 37 $^{\circ}$C, lost activity within 1 week. While when electrodes at 4 $^{\circ}$C analyzed after certain time durations (3 days, 6 days, 9 days etc.), sensitivity of electrodes were found more than 90% of their original response (first day response of nano-octahedra CeO2/Ch/GCE immunosensor at antigen concentration of 25 ng/mL) even after 30 days. In another study, we prepared the PBS buffer solution (antigen and CAb dilution solution) containing 0.1% sodium azide, an additive to prevent fungal growth, for immunosensing purpose. We found that activity of nano-octahedra CeO2/Ch/GCE immunosensor at 4 $^{\circ}$C remained more than 90% of the original activity (first day activity of nano-octahedra CeO2/Ch/GCE immunosensor at antigen concentration of 25 ng/mL) after 51 days. Thermal study of immunosensor was also studied at 37 $^{\circ}$C and 50 $^{\circ}$C.

IV. CONCLUSION

In this present article the amperometric response was found to be linear in the range of 6.25 µg/mL to100 µg/mL with a regression equation of i (nA) = 34.12 + 2.448 x antigen (µg/mL) (R^2=0.999). Detection limit of CE-protein antigen was found 0.1 ng/mL by using CeO2/Ch/GCE. The relative standard deviation was obtained 5.5%. Whereas by ELISA method, the detection limit of CE-protein antigen was 50 µg/mL. The shelf life of immunosensor was found to be 51 days. Post-zone like effect was found in detection of brucellosis. However, no false negative results are obtained by immunosensor. Experiments were also conducted using 110 suspected patient serum samples and results were compared with other standard tests like ELISA & RBPT (Table 1). The immunosensor was found to be more sensitive than standard tests. Thus this immunosensor can be used for diagnosis of brucellosis in patient serum samples. A portable detection system like any hand held potentiostat can be used in field related sensing applications.

V. CONFLICT OF INTEREST STATEMENT

The authors declare no conflict of interest.

VI. ACKNOWLEDGEMENTS

The authors thank Director, D.R.D.E. Gwalior for his continued support in the completion of this study.

REFERENCES

[1] L.G. Andrey, A. Plamen, W. Michael, and W. Ebtisam, "Immunosensor: electrochemical sensing and other engineering approaches", Biosens. Bioelectron, vol. 13, 1998. pp. 113–131.

[2] M. Worwood, "Serum transferrin receptor assay and their application", Ann. Clin. Biochem., vol. 39, 2002, pp. 221–230.

[3] A.K. Trull, "The clinical validation of novel strategies for monitoring transplant recipient", Clin. Biochem., vol. 34, 2001, pp. 3–7.

[4] K. Sato, A. Hibara, M. Tokeshi, H. Hisamoto, and T. Kitamori, "Microchip based chemical and biochemical analysis system", Adv. Drug Deliv. Rev., vol. 55, 2003, pp. 379–391.

[5] J. Rossier, F. Reymond, and P.E. Michel, "Polymer microfluidic chips forelectrochemical and biochemical analysis", Electrophoresis, vol. 23, 2002, pp. 858–867.

[6] H.X. Ju, G.F. Yan, F. Chen, and H.Y. "Enzyme linked immuno assay of α-1-fetoprotein in serum by differential pulse voltammetry", Chen, Electroanalysis, vol. 11, 1999, pp. 124–128.

[7] D.A. Palmer, and J.N. Miller, "Thiophilic gels: applications in flow injection immunoassay for macromolecules and haptens", Anal. Chim. Acta, vol. 303, 1995, pp. 223–230.

[8] M. Nilsson, H. Hakason, and B. Mattiasson, "Process monitoring by flow injection immunoassay evolution of a sequential competitive binding assay", J. Chromatogr., vol. 597, 1992, pp. 383–389.

[9] X. Pang, D. He, S. Luo, and Q. Cai, "An amperometric glucose biosensor fabricated with Pt nanoparticle-decorated carbon nanotubes/TiO_2 nanotube array composite", Sens. Actuators B, vol. 137, 2009, pp. 134-138.

[10] C. Deng, F. Qu, H. Sun, and M. Yang, "Sensitive electrochemical immunosensor based on enlarge and surface charged gold nanoparticles mediated electron transfer", Sens. Actuators B, vol. 160, 2011, pp. 471-474.

[11] Z-M. Liu, Y. Yang, H. Wang, Y-L. Liu, G-L. Shen, and R-Q. Yu, "A hydrogen peroxide biosensor based on nano Au/PAMAM dendrimer/cystamine modified gold electrode", Sens. Actuators B, vol. 106, 2005, pp. 394-400.

[12] S. Chen, R. Yuan, Y. Chai, Y. Xu, L. Min, and N. Li, "A new antibody immobilization technique based on organic polymers protected Prussian blue nanoparticles and gold nanoparticles for amperometric immunosensors", Sens. Actuators B, vol. 135, 2008, pp. 236-244.

[13] R. Khan, A. Kaushik, P.R. Solanki, A.A. Ansari, M.K. Pandey, and B.D. Malhotra, "Zinc oxide nanoparticles-chitosan composite film for cholesterol biosensor", Anal. Chim. Acta, vol. 616, 2008, pp. 207-213.

[14] S. Suresh, A.K. Gupta, V.K. Rao, OmKumar, and R. Vijayaraghvan, "Amperometric immunosensor for ricin by using on graphite and carbon nanotube paste electrodes", Talanta, vol. 81, 2010, pp. 703-708.

[15] S. Vetcha, I. Abdel-Hamid, P. Atanasov, D. Ivnitski, and B. Hjelle, "Portable Immunosensor for the Fast Amperometric Detection of Anti-Hantavirus Antibodies", Electroanalysis, vol. 12, 2000, pp. 1034-1038.

[16] G.J. Renukaradhya, S. Isloor, J.R. Crowther, M. Robinson, and M. Rajasekhar, "Development and field validation of an avitin-biotin enzyme linked immunosorbent assay kit for bovine brecellosis", Rev. Sci. Tech., vol. 20, 2001, pp. 749-756.

[17] P.C. Baldi, G.H. Giambartolomei, F.A. Goldbaum, L.F. Abdon, C.A. Velikovsky, and R. KIttelberger, "Humoral immune response against lipopolysaccharide and cytoplasmic proteins of *Brucella abortus* in cattle vaccinated with B. abortus S19 or experimentally infected with Yesinia enterocolitica serotype O:9", Clin. Diagn. Lab. Immunol., vol. 3 1996, pp. 472-476.

[18] G. Dubray, "Antigens of diagnostic significance on *Brucella"*, In: Verger JM, Plommet M. editors. Brucellla melitensis, a CEE seminar. The Hague, The Netherlands: Martinus Nijhooff Publishing (1985) 123-38.

[19] J.P. Connolly, D. Comerci, T.G. Alefantis, A. Walz, M. Quan, R. Chafin, P. Grewal, C.V. Mujer, R.A. Ugalde, and V.G. DelVecchio, "Proteomic analysis of *Brucella abortus* cell envelope and identification of immunogenic candidate proteins for vaccine development", Proteomics, vol. 6, 2006, pp. 3767–3780.

[20] K. Nielsen, "Diagnosis of brucellosis by serology", Vet Microbiol., vol. 90, 2002, pp. 447-459.

[21] H.A. Al-Shamahy, and S.G. Wright," Enzyme linked immunosorbent assay for *Brucella* antigen detection in human sera", J. Med. Microbiol., vol. 47, 1998, pp. 169-172.

[22] M.I. Al-Farwachi, B.A. Al-Badrani, and Th.M. Al-Nima, "Detection of *Brucella* antigen in the aborted ovine fetal stomach contents using a modified ELISA test", Iraqi Journal of Veterinary Sciences, vol. 24, 2010, pp. 1-4.

[23] M. Sozmen, S.D. Erginsoy, O. Genc, E. Beytut, and A. Ozcan, "Immunohistochemical and Microbiological Detection of *Brucella abortus* in aborted bovine fetuses", Acta Vet. BRNO vol. 73, 2004, pp. 465–472.

[24] J.P.M. Quezada, J. Lopez, O. Casquet, M.A. Sierra, and J.M.dl. Mulas, "Immunohistochemical detection of Brucella abortus antigens in tissues from aborted bovine fetuses using a commercially available polyclonal antibody", J. Vet. Diagn. Invest., vol. 10, 1998, pp. 17–21.

[25] M.P. Franco, M. Mulder, R.H. Gilman, and H.L. Smits,"Human brucellosis", The Lancet infectious diseases, vol. 7, 2007, pp. 775-786.

[26] M.J. Corbel, "The direct fluorescent antibody test for detection of *Brucella abortus* in bovine abortion material", J. Hyg. Camb., 71, 1973, pp. 123-129.

[27] V. Weynants, K. Walravens, C. Didembourg, P. Flanagan, J.J. Godfroid, and J.J. Letesson, "Quantitative assessment by flow cytometry of T-lymphocytes producing antigen-specific γ-interferon in *Brucella* immune cattle", Veterinary Immunology and Immunopathology, vol. 66, 1998, pp. 309-320.

[28] A. Kaushik, P.R. Solanki, A.A. Ansari, S. Ahmad, and B.D. Malhotra, "A nanostructured cerium oxide film based immunosensor for mycotoxin detection", Nanotechnol., vol. 20, 2009, pp. 055105.

[29] A. Kaushik, P.R. Solanki, A.A. Ansari, S. Ahmad, and B.D. Malhotra, "Chitosan-Iron Oxide Nanobiocomposite Based Immunosensor for Ochratoxin-A", Electrochem. Commun., vol. 10, 2008, pp. 1364-1368.

[30] P.R. Solanki, A. Kaushik, A.A. Ansari, and B.D. Malhotra, "Nanostructured ZnO film for cholesterol biosensor", Appl. Phys. Lett., vol. 94, 2009, pp. 143901.

[31] A.A. Ansari, A. Kaushik, P.R. Solanki, and B.D. Malhotra, "Sol-del derived nanoporous cerium oxide film for application to cholesterol biosensor", Electrochem. Commun., vol. 10, 2008, pp. 1246-1259.

[32] S.P. Singh, S.K. Arya, P. Pandey, B.D. Malhotra, S. Saha, K. Sreenivas, and V. Gupta, "Cholesterol biosensor based on rf sputtered Zinc oxide nanoporous thin film", Appl. Phys. Lett., vol. 91, 2007, pp. 063901.

[33] A. Wei, X.W. Sun, J.X. Wang, Y. Lei, X.P. Cai, C.M. Li, Z.L. Dong, and W. Huang, "Enzymatic glucose biosensor based on ZnO nanorod array grown by hydrothermal decomposition", Appl. Phys. Lett., vol. 89, 2006, pp. 123902.

[34] G.K. Kouassi, J. Irudayaraj, and G.J. McCarty, "Examination of Cholesterol oxidase attachment to magnetic nanoparticles", Nanobiotechnol., vol. 3, 2005, pp. 1–9.

[35] A.A. Ansari, P.R. Solanki, and B.D. Malhotra, "Sol-gel derived nanostructured cerium oxide film for glucose sensor", Appl. Phys. Lett., vol. 92, 2008, pp. 263901.

[36] S. Saha, S.K. Arya, S.P. Singh, K. Sreenivas, B.D. Malhotra, and V. Gupta, "Nanoporous cerium oxide thin filmfor glucose biosensor", Biosens. Bioelectron., vol. 24, 2009, pp. 2040-2045.

[37] S.H. Choi, S.D. Lee, J.H. Shin, J. Ha, H. Nam, and G.S. Cha, "Amperometric biosensors employing an insoluble oxidants as an interference-removing agents", Anal. Chim. Acta, vol. 461, 2002, pp. 251-260.

[38] A. Mehta, S. Patil, H. Bang, H.J. Cho, and S. Seal, "A novel multivalent nanomaterial based hydrogen peroxide sensor", Sens. Actuators A, vol. 134, 2007, pp. 146-151.

[39] X. Xiao, Q. Luan, and X. Yao, "Single crystal cerium oxide nanocubes used for the direct electron transfer and electrocatalysis of horseradish peroxidase", Biosens. Bioelectron., vol. 24, 2009, pp. 2447-2451.

[40] W. Zhang, T. Yang, X. Zhuang, Z.G.K. Guo, and K. Jiao, "An ionic liquid supported CeO_2 nanoshuttles-carbon nanotubes composite as a plateform for impedance DNA hybridization sensing", Biosens. Bioelectron., vol. 24, 2009, pp. 2417-2422.

[41] K.J. Feng, Y.H. Yang, Z.J. Wang, J.H. Jiang, G.L. Shen, and R.Q. Yu, "A nanoporous CeO_2/chitisan nanocomposite film as a immobilization matrix for colorectal cancer DNA sequence-selective electrochemical biosensor", Talanta, vol. 70, 2006, pp. 561-565.

[42] B.D. Malhotra, and A. Kaushik, "Metal oxide-chitosan based nanocomposite for cholesterol biosensor", Thin Solid Films, vol. 518, 2009, pp. 614-620.

[43] S.S. Lin, C.L. Chen, D.J. Chang, and C.C. Chen, "Catalytic wet air oxidation of phenol by various CeO2 catalysts", Water Res. vol., 36, 2010, pp. 3009-3014.

[44] S. Hamoudi, F. Larachi, G. Cerrella, and M. Cassanello, "Wet Oxidation Of Phenol Catalyzed By Unpromoted And Platinum-Promoted Manganese Cerium Oxide", Ind. Eng. Chem. Res., vol. 37, 1998, pp. 3561-3566.

[45] C. Zengxiong, Z. Wanpeng, Y. Shaoxia, and W. Jianbing, "Preparation and characterization of TiO_2-CeO_2 catalyst for catalytic wet air oxidation of phenol", Chin. J. Catal., vol. 27, 2006, pp. 1073-1079.

[46] L.F. Pease III, J.T. Elliott, D-H. Tsai, M.R. Zachariah, and M. Tarlov, "Determination of protein aggregation with differential mobility analysis: application to IgG antibody", J. Biotechnol. Bioengineering, vol. 101, 2008, pp. 1214-1222.

[47] A.K. Gupta, V.K. Rao, D.T. Selvam, A. Kumar, and R. Jain, "Amperometric immunosensor of brucella abortus CE-protein antigen shows post-zone phenomenon", J. Electroanal. Chem., vol. 717-718, 2014, pp. pp. 83-89.

[48] C. Xu, H. Cai, P. He, and Y. Fang, "Electrochemical detection of sequence-specific DNA using a DNA probe labeled with aminoferrocene and chitosan modified electrode immobilized with ssDNA", Analyst, vol. 2001, pp. 126, 62.

[49] H. Yorgancigil, G. Yayli, and O. Oyar, "Neglected case of *Brucella* infection of the knee", Croat. Med. J., vol. 44, 2003, pp. 761-763.

[50] M-M. Titirici, M. Antonietti, and A. Thomas, "Engineering carbon materials from the hydrothermal carbonization process of biomass", Chem. Mater., vol. 18, 2006, pp. 3808-3812.

[51] D. Yang, Z. Han, D. Ma, H. Liang, L. Liu, and Y. Yang, "Fabrication of Monodisperse CeO_2 Hollow Spheres Assembled by Nano-octahedra", Crystal growth and design, vol. 10, 2010, pp. 291-295.

[52] O. H. Lowry, N.J. Rosebrough, A.L. Farr, and R.J. Randall, "Protein measure with the folin phenol reagent", J. Biol. Chem., vol. 193, 1951, pp. pp. 25-275.

[53] M.P. Chatrathi, J. Wang, and G.E. Collins, "Sandwich electrochemical immunoassay for the detection of Staphylococcal enterotoxin B based on immobilized thiolated antibodies", Biosens. Bioelectron., vol. 22, 2007, pp. 2932-2938.

[54] M. Zawadzki, "Preparation and characterization ceria nanoparticlesby microwave assisted solvothermal process", J. Alloys Compd., vol. 454, 2008, pp. 347-351.

[55] J.R. McBride, K.C. Hass, B.D. Poindexter, and W.H. "Raman and X-ray studies of $Ce_{1-x}REx O_{2-y}$", Weber, J. Appl. Phys., vol. 76, 1994, pp. 2435-41.

[56] P. Fornansiero, G. Balducci, R. Dimonte, J. Kasper, V. Sergo, G. Gubitosa, A. Ferrero, and M. Graziani, "Modification of redox behavior of CeO_2 induced by structural doping with ZrO_2", J. Catal., vol. 164, 1996, pp. 173-183.

[57] P. Plackett, and G.G. Alton, "A mechanism for prozone formation in the complement fixation test for bovine brucellosis", Austral. Vet. J., vol. 51, 1975, pp. 374-377.

[58] H. J. Cho, and D.G. Ingram, "Mechanisms of prozone formation in agglutination reaction", Can. J. Microbiol., 1972, vol. 18, 449-456.

[59] S.C. Bruins, I. Ingwer, M.L. Zeckel, and A.C. White, "Parameters affecting the enzyme-linked immunosorbent assay of immunoglobulin G antibody to a rough mutant of Salmonella Minnesota", Infect. Immun., vol. 21, 1978, pp. 721-728.

[60] J.G. Vos, J. Buys, J.G. Hanstede, and A.M. Hagenaars, "Comparison of enzyme-linked immunosorbent assay and passive hemagglutination method for quantitation of antibodies to lipopolysaccharide and tentanus toxoid in rats", Infect. Immun., vol. 24, 1979, pp. 798-803.

[61] V.L. Lamb, L.M. Jones, G.G. Schurig, and D.T. "Enzyme-linked immunosorbent assay for bovine immunoglobulin subclass-specific response to *Brucella abortus* lipopolysaccharides", Berman, Infect. Immun., vol. 26, 1979, pp. 240-247.

[62] K. Malkin, "Enhancement of Leptospira hardjo agglutination titers in sheep and goat serum by heat inactivation", Can. J. Comp. Med., 48, 1984, pp. 208-210.

[63] K.R. Mittal, and I.R. Tizard, "Agglutination tests and their modifications in the diagnosis of bovine brucellosis", Comparative Immunol. Microbiol. Infect. Diseas., vol. 6, 1983, pp. 1-8.

[64] L.G. Hefter, M.A. Hix, M.E. Stoner, and C.B. Cook, "False negative hepatitis B surface antigen detection in dialysis patients due to excess surface antigen: postzone phenomenon", J. Clin. Pathol., vol. 33, 1980, pp. 993-994.

[65] T. Sato, H. Fujita, Y. Ohara, and M. Homma, "Microagglutination test for early and specific serodiagnosis of Tularemia", J. Clin. Microbiol., vol. 28, 1990, pp. 2372-2374.

[66] S. Tiwari, A. Kumar, D.T. Selvam, S. Mangalgi, V. Rathod, A. Prakash, A. Barua, S. Arora, and K. Sathyaseelan, Clin. Vaccin. Immunol., vol. 20, 2013, pp. 1217-1222.

[67] G.G. Alton, L.M. Jones, and D.E. Pietz, "Laboratory technique in brucellosis", second ed., world health organization, Geneva, Switzerland, 1975.

Captions of Fig./Scheme/Table

Fig. 1. SEM image of prepared nano-octahedra CeO_2.
Fig. 2(a). Determination of composition ratio of CeO_2 and Chitosan by means of redox couple (1mM of ferricyanide/ferrocyanide redox couple in PBS).
Fig. 2(b). Determination of composition ratio of CeO_2 and Chitosan by means of 0.5 mM 1-naphthol in DEA buffer.
Fig. 2(c). Comparative CV of GCE and CeO_2/Ch modified GCE in 0.5 mM 1-naphthol (in DEA) (Red curve indicate CeO_2/Ch modified GCE and blue curve indicate GCE.
Fig. 2(d). Amperometric response of GCE and CeO_2/Ch/GCE with subsequent addition of 20 µL of 0.5 mM 1-naphthol (in DEA). (Red curve indicate CeO_2/Ch/GCE and blue curve indicate GCE). Each addition of 20 µL of 0.5 mM 1-naphthol in 10 mL of DEA solution corresponds to concentration of 1 µM.
Fig. 3(a). Relative ALP adsorption efficiency of SPE, MWCNT-paste electrode, ZnO modified SPE and CeO_2 modified GCE.
Fig. 3b). Nyquist plot of EIS in a solution containing 1 mM $Fe(CN)_6^{3-/4-}$ with 0.1 M KCl at 0.20 V (frequency range 0.1 Hz-10 kHz). (a) represents the spectra of unmodified GCE. (b) represents the spectra of chitosan modified GCE and (c) represents the spectra of CeO_2/chitosan modified GCE.
Fig. 4. Optimization of ALP enzyme tagged antibody (RAb) dilution.
Fig. 5. Calibration curve for the concentration of CE-Antigen vs. current for nano-octahedra CeO_2/Ch/GCE. **(a)** depicts the linear range from 6.25 µg/mL to 100 µg/mL. **(b)** depicts the detection limit of 0.1 ng/mL.
Graphical Abstract. Schematic diagram of immunoassay Procedure.
TABLE 1. Comparing results of 110 patient serum sample analysis done by amperometric method (using CeO_2/Ch/GCE immunosensor) and other biological methods such as ELISA method and RBPT Test. Analysis was done by both mean without serum sample dilution and with serum sample dilution.

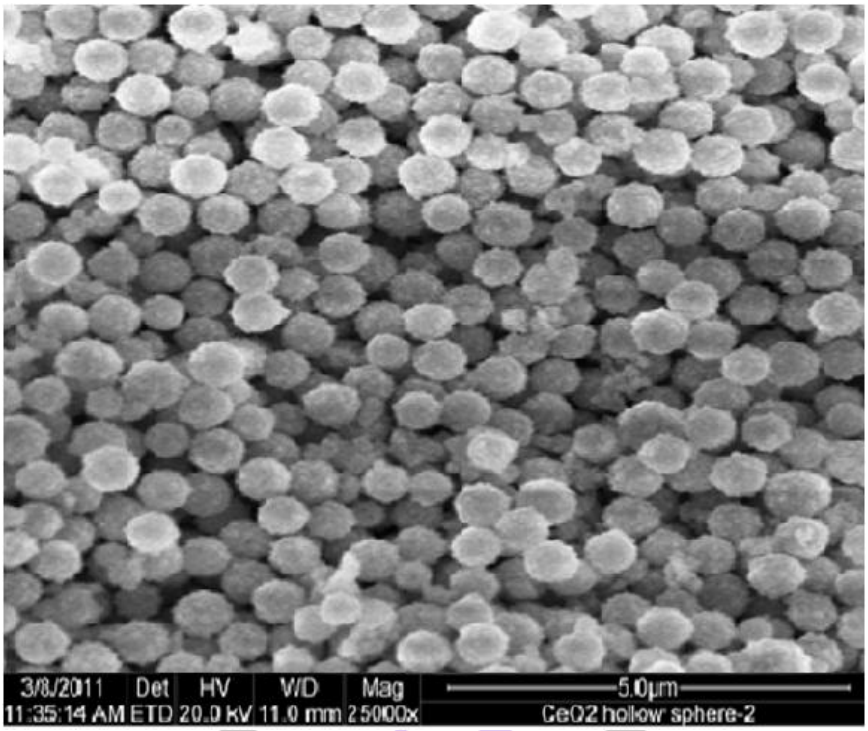

Fig. 1. SEM image of prepared CeO_2 nano-octahedra

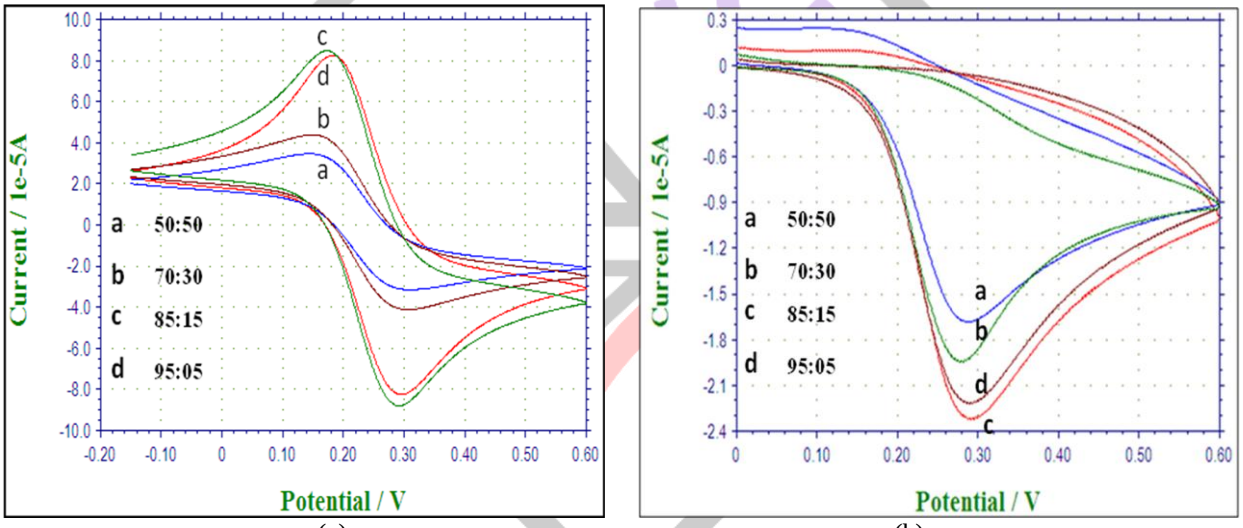

(a) (b)

Fig. 2(a) Determination of composition ratio of CeO_2 and Chitosan by means of redox couple (1mM of ferricyanide/ferrocyanide redox couple in PBS**).**

Fig. 2(b) Determination of composition ratio of CeO_2 and Chitosan by means of 0.5 mM 1-naphthol

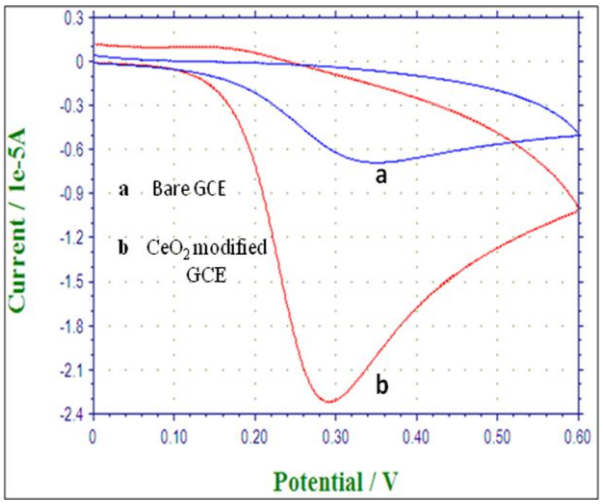

(c)

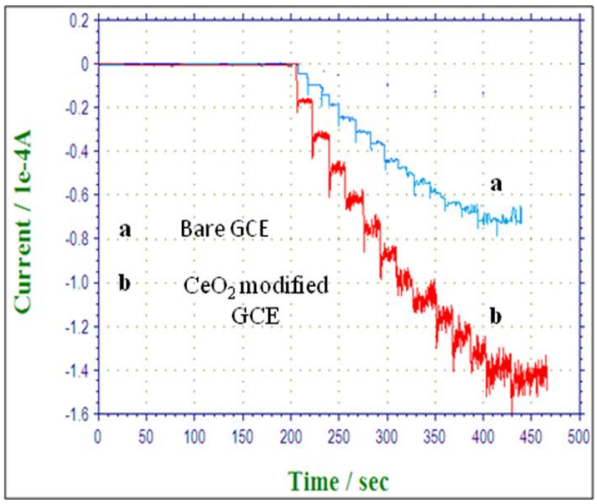

(d)

Fig. 2(c). Comparative CV of GCE and CeO_2/Ch modified GCE in 0.5 mM 1-naphthol (in DEA) (Red curve indicate CeO_2/Ch modified GCE and blue curve indicate GCE.

Fig. 2(d). Amperometric response of GCE and CeO_2/Ch/GCE with subsequent addition of 20 µL of 0.5 mM 1-naphthol (in DEA). (Red curve indicate CeO_2/Ch/GCE and blue curve indicate GCE). Each addition of 20 µL of 0.5mM 1-naphthol in 10 mL of DEA solution corresponds to concentration of 1 µM.

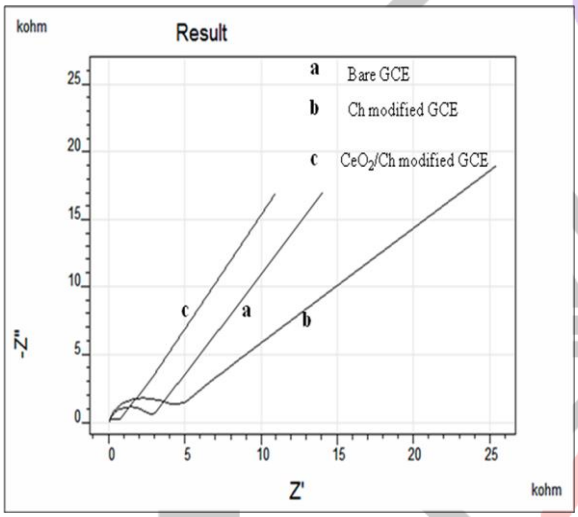

(a)

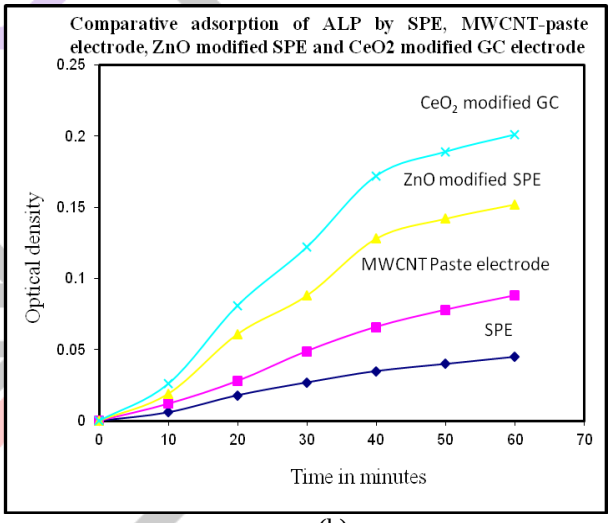

(b)

Fig. 3(a). Relative ALP adsorption efficiency of SPE, MWCNT-paste electrode, ZnO modified SPE and CeO_2 modified GCE.
Fig. 3(b). Nyquist plot of EIS in a solution containing 1mM $Fe(CN)_6^{3-/4-}$ with 0.1M KCl at 0.20 V (frequency range 0.1 Hz-10 kHz). (a) represents the spectra of unmodified GCE. (b) represents the spectra of chitosan modified GCE and (c) represents the spectra of CeO_2/Ch modified GC electrode.

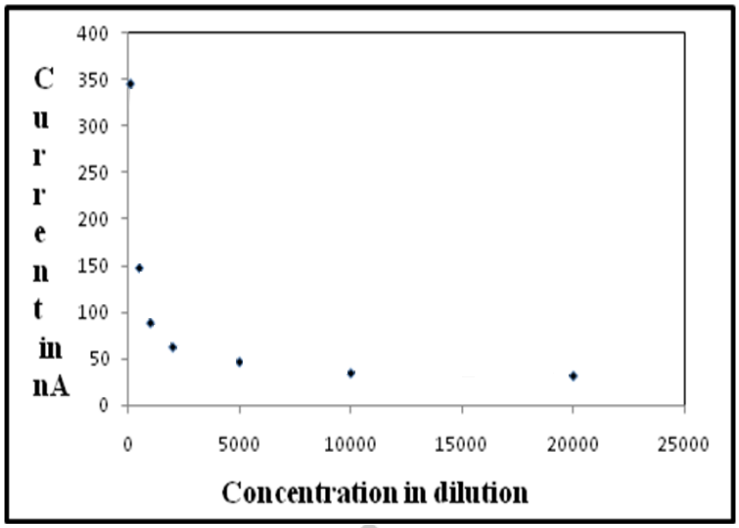

Fig. 4. Optimization of ALP enzyme tagged antibody (RAb) dilution

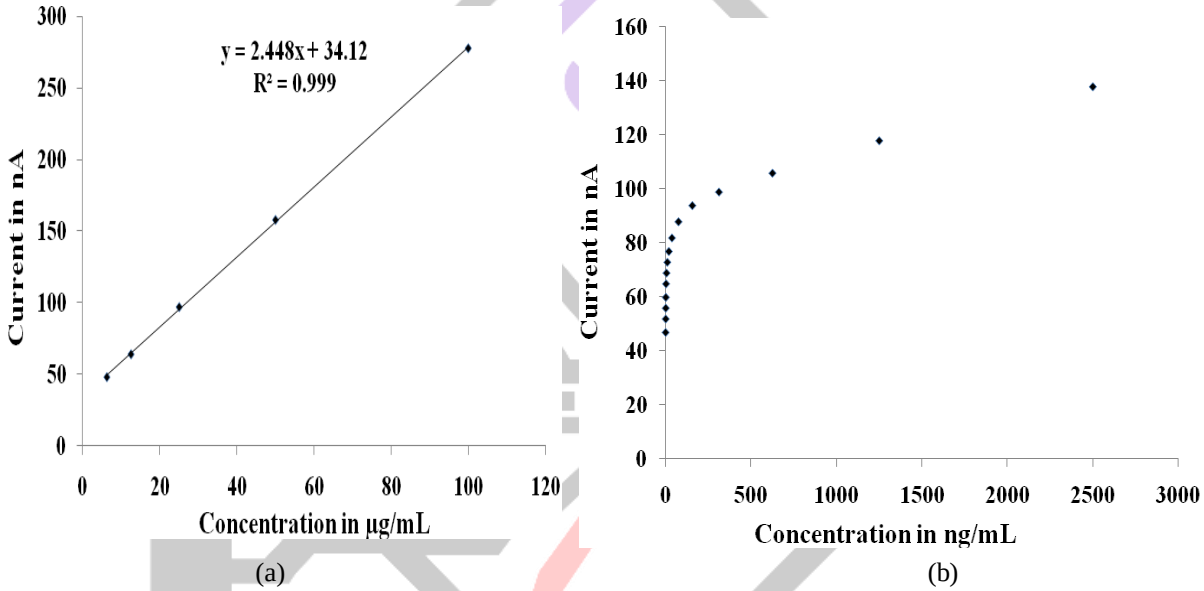

(a) (b)

Fig. 5. Calibration curve for the concentration of CE-Antigen vs. current for nanooctahedra CeO_2/Ch/GCE.
(a) depicts the linear range from 6.25 µg/mL to 100 µg/mL.
(b) depicts the detection limit of 0.1ng/mL.

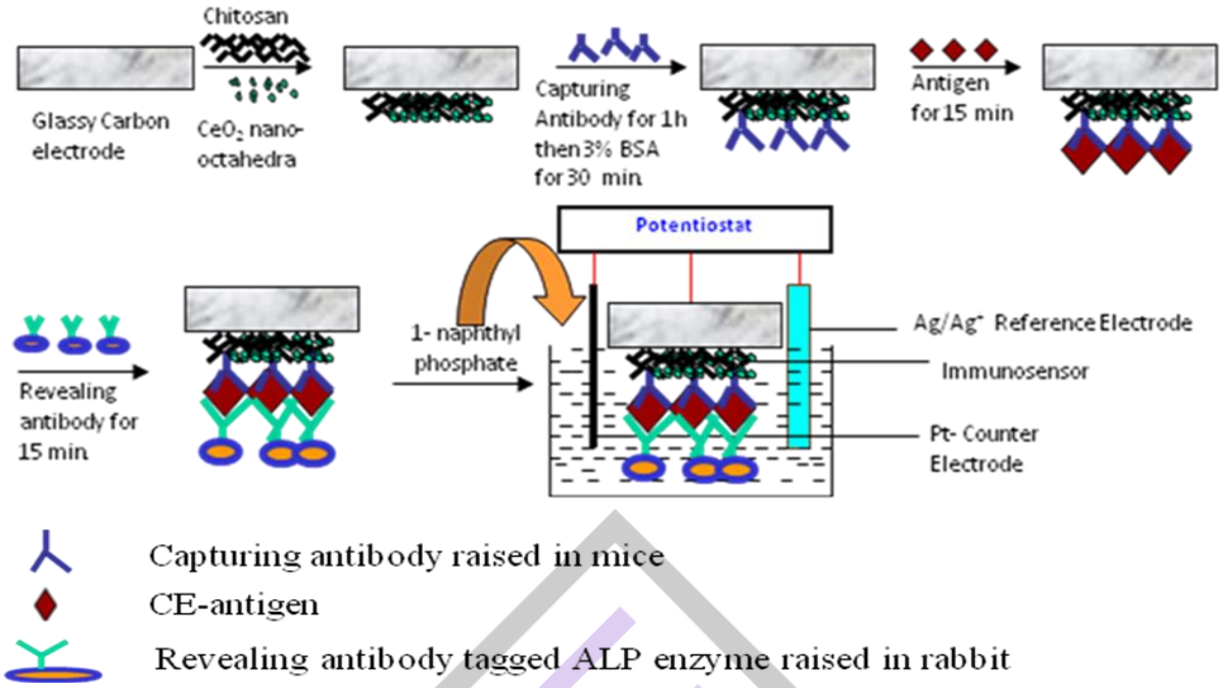

Graphical Abstract. Schematic diagram of immunoassay Procedure.

Table 1

Comparing results of overall patient serum sample analysis done by amperometric method (using CeO_2/Ch/GCE immunosensor) and other biological methods such as ELISA method and RBPT Test. Analysis was done by both mean without serum sample dilution and with serum sample dilution.

	Culture	Without Sample Dilution			
		ELISA Method		RBPT Test	Electrochemical Methods (Antigen Detection)
		Antigen Detection	Antibody Detection		
No. of positive Samples	19	28	39	48	75
No. of Negative Samples	91	82	71	62	33
No. of unclear Samples	-	-	-	-	02
Total No. of Samples	110	110	110	110	110
Samples diluted 10 times					
No. of Positive Samples	-	00	12	00	32
No. of Negative Samples	-	110	98	110	18